Parameter Identification and Automatic Control Loop Tuning for PMAC Servo Motor Drives

Sheng-Ming Yang, Jin-De Lin, and Kuang-Wei Lin
Department of Electrical Engineering
National Taipei University of Technology
Taipei, Taiwan

***Abstract*—High performance servo motor drives generally consisted of current, velocity, and position control loops. Tuning these controllers to achieve satisfactory and consistent dynamic responses is important. In this paper, a parameter identification and auto-tuning scheme for PMAC servo motor drives is presented. Motor electrical parameters such as resistance and inductances are identified first for current control loop tuning. Then, torque constant and mechanical parameters are identified for velocity and position loop tuning. The experimental results verified that the proposed scheme can estimate parameters with good accuracy. Furthermore, depending on the setting of the tuning process, the auto-tune process can be completed within 1.9 seconds. The control system tuned by the proposed scheme can achieve good dynamic performance.**

Keywords—PMSM Servo Motor; Parameters Identification; Auto-Tune.

I. INTRODUCTION

High performance servo motor drives require control loop tuning for commissioning and regular operations in order to maintain a consistent dynamic response. These drives generally consisted of current, velocity, and position control loops. To tune these controllers automatically, electrical and mechanical parameters must be identified along with a feasible procedure and reasonably short execution time.

Many schemes have been proposed to identify controller-related parameters for drive auto-tune in the past. A model-free method was presented which used motor speed response to estimate inertia [1]. Model reference adaptive control was also applied to find drive inertia [2][3]. Some studies proposed to use disturbance observer based auto-tuning schemes. The disturbance estimator has various forms, for example, state estimator [4][5], and Kalman filter [6]. Several researches proposed methods to identify torque constant via motor back-emf [7][8]. These two parameters are required in most estimators and drive tuning. High frequency voltage injection schemes were also applied to identify inductances [9]. However, these schemes only applicable for inductance or resistance identifications. Several parameter identification and estimation schemes are summarized and compared in [10]. Most of these schemes are either cumbersome for implementation or the execution time is too long for practical use.

In this paper, a parameter identification and auto-tuning scheme for permanent magnet ac (PMAC) servo motor drives is presented. Motor electrical parameters such as resistance and inductances are identified first for current control loop tuning. Then, torque constant and mechanical parameters are identified for velocity and position loop tuning. Both theoretical analysis and experimental verifications are presented in the paper.

II. MATHEMATICAL MODEL

The voltage equations of a three-phase permanent magnet ac motor in rotor reference frame can be expressed as

$$v_{qs}^r = \left(r_s + L_{qs} p\right) i_{qs}^r + \omega_r L_{ds} i_{ds}^r + \omega_r \lambda_m \tag{1}$$

$$v_{ds}^r = \left(r_s + L_{ds} p\right) i_{ds}^r - \omega_r L_{qs} i_{qs}^r \tag{2}$$

where v_{qs}^r, v_{ds}^r, i_{qs}^r and i_{ds}^r are the q- and d-axis voltages and currents, r_s is the resistance, L_{qs} and L_{ds} are the q- and d-axis inductance, λ_m is the flux linkage established by the rotor permanent magnets, ω_r is the rotor electrical speed, and p represents the differentiator operator (d/dt). Note that from (1), the back-emf constant can be expressed as $K_e = (P/2)\lambda_m$, where P is the number of rotor poles. The generated motor torque is

$$T_e = \frac{3}{2}\frac{P}{2}\left[\lambda_m i_{qs}^r + \left(L_{ds} - L_{qs}\right) i_{qs}^r i_{ds}^r\right] \tag{3}$$

As can be seen in the above expression, d- and q-axis current can be set to follow certain trajectory to achieve maximum torque per ampere or other types of control. However, in this paper, d-axis current is set to zero for convenience. Thus, T_e becomes proportional to the q-axis current, and the motor torque constant can be expressed as

$$K_t = \frac{3}{2}\frac{P}{2}\lambda_m = \frac{3}{2}K_e \tag{4}$$

Also, the mechanical equation can be expressed as

$$T_e = J\frac{d\omega_m}{dt} + B\omega_m + T_L \tag{5}$$

where J is the combined rotor and load inertia, B is the viscous frictional coefficient, ω_m is the mechanical speed, and T_L is the disturbance load torque.

III. MOTOR CONTROLLERS

Servo motor drive is generally consisted of two inner current control loops (q- and d- axis), a speed control loop, and an outer position control loop. Conventional linear regulators are usually used for these loops. Figure 1 shows the schematic of the control systems. This section describes how the loop gains are determined from motor parameters.

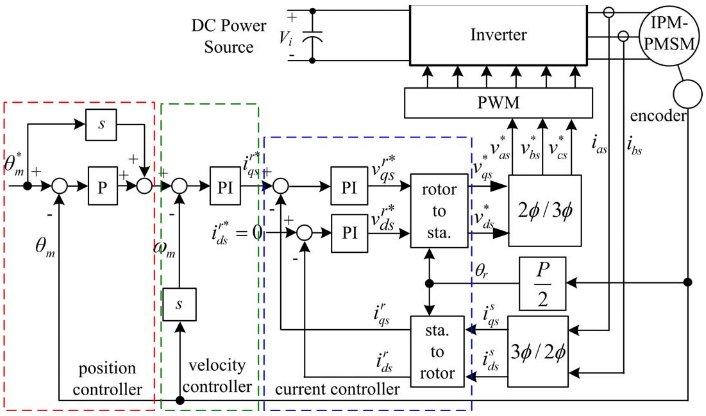

Fig. 1 Motor control system.

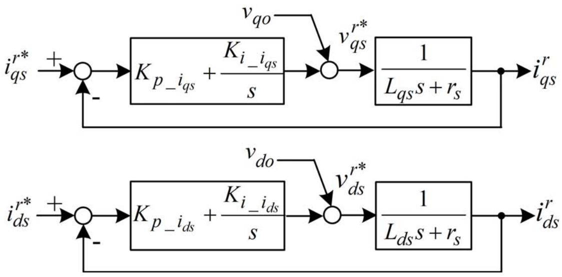

Fig. 2 q- and d-axis current controllers.

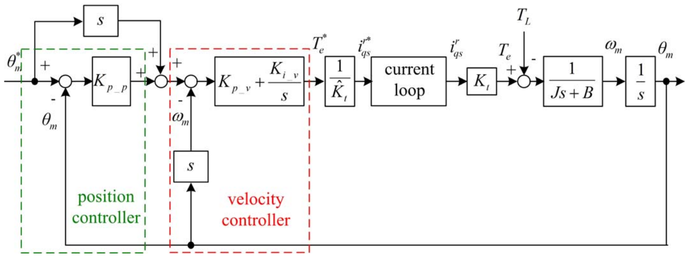

Fig. 3 Simplified motor control system.

A. Current Controllers

The schematic of the current controllers are shown in Fig. 2, proportional plus integral (PI) regulators are used. The cross-coupling voltages and the back-emf voltages are decoupled using the estimated electrical parameters and rotor speed. The decoupling voltages, i.e. v_{qo} and v_{do}, are also shown in Fig. 2.

Ratio between the proportional and integral gain is setup to cancel the *r*-*L* pole. For example in the q-axis, the gain ratio is set to: $K_{p\_iqs} / K_{i\_iqs} = L_{qs} / r_s$, where K_{p_iqs} and K_{i_iqs} are the proportional and the integral gain, respectively. After the cancellation, q-axis closed-loop transfer function can be expressed as

$$\frac{i_{qs}^{r}(s)}{i_{qs}^{r*}(s)} = \frac{K_{p\_iqs} / L_{qs}}{s + K_{p\_iqs} / L_{qs}} = \frac{\omega_{iq}}{s + \omega_{iq}} \tag{6}$$

where ω_{iq} is the bandwidth of the q-axis current controller, its value can be set according to the desired bandwidth of the controller. The gains can be expressed as

$$K_{p\_iqs} = \omega_{iq} \cdot L_{qs} \tag{7}$$

$$K_{i\_iqs} = \omega_{iq} \cdot r_s \tag{8}$$

Note that the d-axis gains can be determined with a similar procedure. Therefore, r_s, L_{qs}, L_{ds} are required to calculate gains of the current controllers.

B. Velocity Controller

As shown in Fig. 1, the velocity and the position control loops are cascaded. Since the bandwidth of the current loop is much higher than the outer control loops, perfect current regulation is assumed for velocity control loop tuning. Figure 3 shows the simplified motor control system.

Let K_{p_v} and K_{i_v} be the proportional and integral gain of the velocity controller, respectively, the velocity response can be expressed as

$$\frac{\omega_m(s)}{\omega_m^*(s)} = \frac{\frac{K_{p\_v}}{J} s + \frac{K_{i\_v}}{J}}{s^2 + \frac{(K_{p\_v} + B)}{J} s + \frac{K_{i\_v}}{J}} \tag{9}$$

If the damping ratio is set to 1 and the bandwidth of the velocity control is ω_v, then the gains can be determined as

$$K_{p\_v} = 2 \cdot \omega_v \cdot J - B \tag{10}$$

$$K_{i\_v} = \omega_v^2 \cdot J \tag{11}$$

Because ω_v is set according to the desired bandwidth, J and B are required to calculate the velocity control loop gains. Also as shown in Fig. 3, torque constant K_t is also required for the conversion between torque command (T_e^*) and current command (i_{qs}^{r*}).

C. Position Controller

Similarly, assuming the bandwidth of the velocity control loop is much higher than that of the position control loop, the position response can be expressed as

$$\frac{\theta_m(s)}{\theta_m^*(s)} = \frac{s + K_{p\_p}}{s + K_{p\_p}} = \frac{s}{s + K_{p\_p}} + \frac{K_{p\_p}}{s + K_{p\_p}} \tag{12}$$

where K_{p_p} is gain as well as the bandwidth of the control loop, and it is set according to the desired bandwidth of the position control.

IV. ELECTRICAL PARAMETER IDENTIFICATION

This section describes identification procedures for electrical parameters. As explained in Section III, tuning current loop gains require resistance and inductances. These parameters are identified under open-loop operations.

A. Stator Resistance (r_s)

To avoid error due to rotor movements, resistance is measured by applying a voltage to the d-axis (V_r), then measure the steady state d-axis current (I_r). Then, the resistance can be calculated as

$$r_s = \frac{V_r}{I_r} \tag{13}$$

Because the voltage is applied at $\theta_r = 0^\circ$ and no q-axis current is produced, rotor will not move.

In the actual implementation, two consecutive voltage pulses are applied to the motor in order to compensate for the voltage error caused by the power switches and diodes. As shown in Fig. 4, these voltage pulses have the same polarity but different magnitudes. The resistance is calculated as

$$\hat{r}_s = \frac{V_{r2} - V_{r1}}{I_{r2} - I_{r1}} \tag{14}$$

Where V_{r1} and V_{r2} are the voltage commands for the resistance estimation, and the symbol with '^' represents measured value.

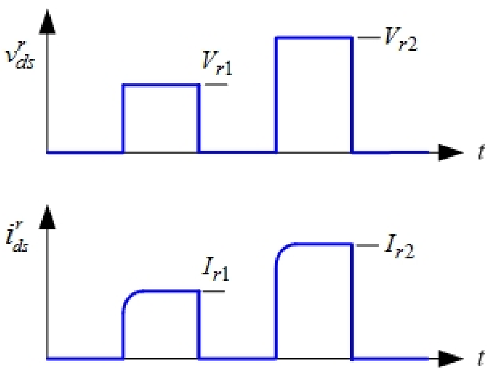

Fig. 4 voltage and current waveforms when measuring resistance.

B. Inductances (L_{ds}, L_{qs})

The inductances are measured by applying voltage pulses to the q- and d-axis, then the peak currents are measured for inductances calculations. Since the time duration for these voltage pulses are very short, typically less than 100μs, the resistance drop and motor movements can be neglected. From (1) and (2) the motor voltages can be approximated as

$$v_{qs}^r \cong L_{qs} p \cdot i_{qs}^r \tag{15}$$

$$v_{ds}^r \cong L_{qs} p \cdot i_{ds}^r \tag{16}$$

Because the currents and the generated torque are small, significant measurement error may occur if the rotor movement is too large. In order to reduce rotor movement the voltage pulses are applied at $\theta_r = 0^\circ$ and the time duration for the d-axis is set to twice as that of the q-axis. Let the time duration for q-axis be h, d-axis time duration be $2h$, then the inductances can be approximated as

$$\hat{L}_{qs} \approx \frac{v_{qs}^r}{\Delta i_{qs}^r} \Delta t = \frac{V_{qs}^r}{\Delta i_{qs}^r} h \tag{17}$$

$$\hat{L}_{ds} \approx \frac{v_{ds}^r}{\Delta i_{ds}^r} \Delta t = \frac{V_{ds}^r}{\Delta i_{ds}^r} 2h \tag{18}$$

where V_{qs}^r and V_{ds}^r are the magnitude of the applied voltages.

Similar to the resistance measurement, in order to reduce errors caused by the inverter circuits, the above test is repeated twice with the same polarity but different magnitude voltage pulses. The differential voltage and current of these two tests are used for inductance calculations as follows,

$$\hat{L}_{qs} \cong \frac{V_{qs2}^r - V_{qs1}^r}{\Delta i_{qs2}^r - \Delta i_{qs1}^r} h \tag{19}$$

$$\hat{L}_{ds} \cong \frac{V_{ds2}^r - V_{ds1}^r}{\Delta i_{ds2}^r - \Delta i_{ds1}^r} 2h \tag{20}$$

where V_{qs1}^r, V_{qs2}^r, V_{ds1}^r and V_{ds2}^r are the voltage commands for the inductance estimation.

Figure 5 shows the schematic of the voltage and current waveforms for inductance measurement. After the resistance and inductances are measures the current controller gains can be calculated with (7) and (8). Note that at this point, v_{qo} and v_{do} can not be set yet since K_t is not known.

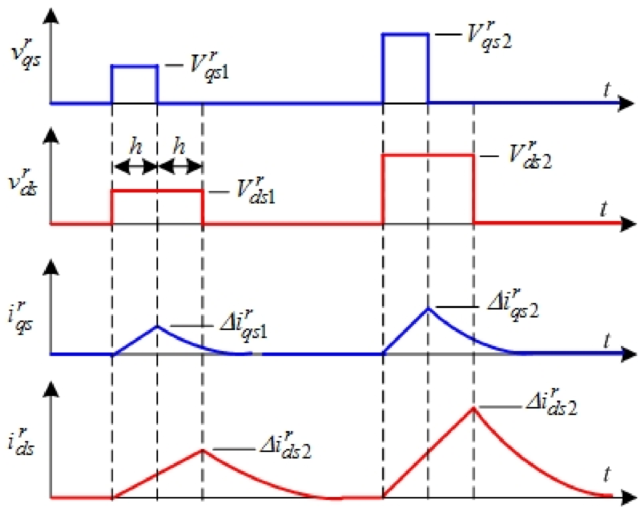

Fig. 5 voltage and current waveforms when measuring inductances.

C. Back-emf and Torque Constants (K_e, K_t)

From the previous sections we know that $K_t = 1.5K_e$, and K_t is needed to determine control gains. In this paper we propose a scheme to estimate K_e, and then use the measured K_e to calculate K_t. During the estimation rotor must rotate to a steady speed. If the influence from PWM is neglected and i_{ds}^r is set to zero, the q-axis voltage can be rewritten as

$$v_{qs}^r = (r_s + L_{qs} \cdot s) i_{qs}^r + \omega_r \lambda_m \tag{21}$$

Substituting λ_m with K_t, the back-emf constant can be expressed as

$$\hat{K}_e = \frac{\omega_r \hat{\lambda}_m}{\omega_m} = \frac{v_{qs}^r - i_{qs}^r (\hat{L}_{qs} \cdot s + \hat{r}_s)}{\omega_m} \tag{22}$$

Therefore, K_e can be estimated from the q-axis voltage, current, and motor speed.

Figure 6 shows the block diagram of the q-axis current controller and the K_e estimator. Note that voltage command (v_{qs}^{r*}) is used instead of the actual voltage in the estimator. As shown in the figure, accuracy of the estimated K_e is dependent to the current control error. Unfortunately, as explained in Section II, current controllers require decoupling voltages v_{qo} and v_{do} to reduce transient errors, and these voltages are not yet available when estimating K_e. Therefore, the estimation is implemented in two steps, first setup proper de-coupling voltage, and then estimate K_e.

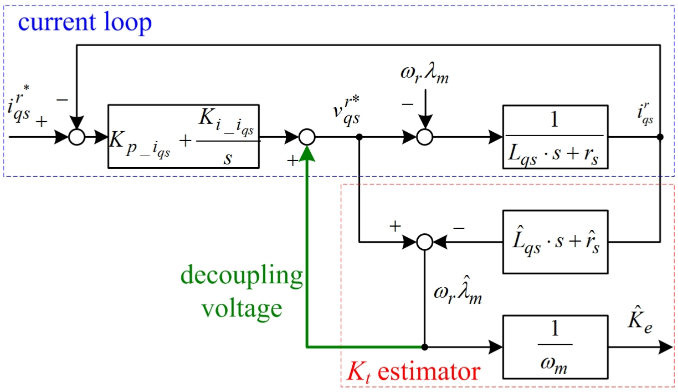

Fig. 6 Current controller and the torque constant estimator.

Referring to Fig. 7, current controller gains are set to the values determined by (7) and (8) before $t = t_0$. In order to limit motor speed the current command is set to a preset value i_1 and the q-axis current gain $K_{i\_i_{qs}}$ is set to 0. Because the decoupling voltage $v_{qo} = 0$, i_{qs}^r will rise first, and then drop down to a value as speed settles down to ω_1. As shown in Fig. 6, after i_{qs}^r reached steady state $\omega_r \hat{\lambda}_m$ is equivalent to $v_{qs}^{r*} - i_{qs}^r (\hat{L}_{qs} \cdot s + \hat{r}_s)$, which is the q-axis de-coupling voltage v_{qo}.

At $t = t_2$, v_{qo} and v_{do} are calculated and then established in the current controller. Due to the addition of this voltage motor accelerates up toward ω_2 and current tracking error is reduced at the same time. Consequently, $\hat{K}_e$ can be calculated with good accuracy after rotor settled down.

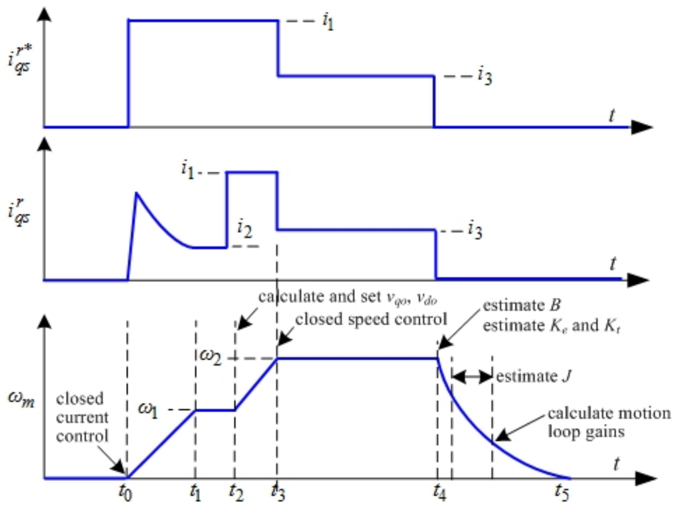

Fig. 7 Waveforms when measuring K_e, K_t, J, and B.

V. MECHANICAL PARAMETER IDENTIFICATION

Again as shown in Fig. 7, at $t = t_3$, speed control loop is closed and its command set to ω_2. Because the mechanical parameters are not available yet, velocity control gains are set empirically. One simple setting is to let $K_{p\_v} = 0$ and $K_{i\_v} = 1$. Because the velocity controller is activated when motor is running, depending on the controller rotor may oscillate for a period of time. Average i_{qs}^r is calculated and denoted as i_3. As motor reached steady state, i.e. $t = t_4$, B can be found as

$$\hat{B} = \frac{\hat{K}_t \cdot i_3}{\omega_2} \tag{23}$$

After B is estimated all the controllers are switched off and the motor decelerated down to zero speed. Note that $\hat{K}_e$ and $\hat{K}_t$ are also calculated at $t = t_4$.

Rotor inertia can be calculated with the current, speed, and the acceleration rate during [t_2, t_3] or with the velocity waveform during [t_4, t_5] region via curve fitting. To calculate using the acceleration rate, neglecting T_L and from (5),

$$\hat{K}_t \cdot i_1 = \hat{J} \cdot \alpha_m + \hat{B} \cdot \omega_m = \hat{J} \cdot \frac{\omega_2 - \omega_1}{t_3 - t_2} + \hat{B} \cdot \omega_2 \tag{24}$$

However, it was found that using curve fitting gave results closer to the theoretical value than using (24). This may have been due to the current measurement errors as the motor is in acceleration.

After $\hat{J}$ and $\hat{B}$ are measured the velocity and position control gains can be calculated with (10)-(11) and (12), respectively. The auto-tune process completed and the motor drive is ready for servo operations. Figure 8 shows the flowchart of the parameter identification and controller gain tuning processes.

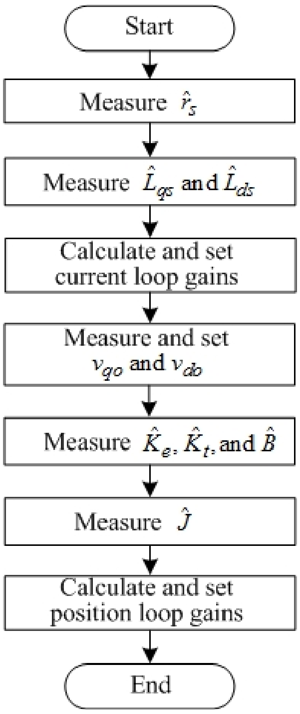

Fig. 8 Flowchart of the auto-tuning process.

I. EXPERIMENTAL RESULTS

A 400W, 8-pole IPM-PMSM was used for experimental verification of the proposed auto-tune scheme. Motor controllers are implemented with a DSP. Manually measured motor parameters are given in Table 1. Magnitudes of the voltage pulses for resistance measurement are 3.1V and 4.8V, respectively, and the pulses width is 62.5ms. Magnitude of the voltage pulses for q-axis inductance measurement are 25V and 50V, the d-axis are 21V and 43V, and the pulse width h = 55μs. The current loop bandwidth (ω_{iq} and ω_{id}), the velocity loop bandwidth (ω_v), and the position loop bandwidth are set to about 500Hz, 50Hz, and 5Hz, respectively.

Figure 9 shows the q-axis, d-axis current, and speed waveforms for the auto-tune process when K_{p_v} and K_{i_v} during [t_3, t_4] are set to 0 and 1, respectively. Figure 10 is the amplified view of the r_s and L measurement waveforms. The two larger pulses are the resistance measuring pulses, and the following two smaller pulses are for inductance measuring pulses. As shown in these figures, the r_s and L measurements take about 0.5 seconds, and the K_t, J and B measurements take about 6.3 seconds. The whole auto-tune process takes about 6.8 seconds for completion.

As mentioned in Section V, K_{p_v} and K_{i_v} during [t_3, t_4] are selected arbitrarily as long as speed can be stabilized with no steady state error. Therefore, various K_{p_v} and K_{i_v} combinations are also tested, and the results are shown in Figs. 11-12. Note that the final K_{p_v} and K_{i_v} calculated with (10) and (11) are 0.16 and 11, respectively. It can be seen from these results that addition of the proportional gain had helped to stabilize the rotor faster and reduced measurement time. As shown in Fig. 12, the whole auto-tune process takes about 1.9 seconds when K_{p_v} and K_{i_v} during [t_3, t_4] are set to 0.16 and 10, respectively.

The parameters identified with the proposed scheme are consistent for various measurement settings described above. Table 1 shows the average of five measurements. The errors between manual and auto-identified parameters are also shown in the table with the manual values as the basis. It can be seen that most parameter errors are within 10%. However, r_s and L_{ds} have much larger errors. These errors may have been caused by the variation of power switch voltages during testing.

II. CONCLUSION

An auto-tuning scheme for the controllers of PMSM servo motor drives is presented in this paper. Dependent on the parameter to be measured the controller sends out proper signals to the motor to identify its value. The servo control loop gains are tuned automatically with the identified parameters. The experimental results verified that the proposed scheme can estimate parameters with good accuracy. Furthermore, depending on the setting of the tuning process, the auto-tune process can be completed within 1.9 to 6.8 seconds. The control system tuned by the proposed scheme can achieve good dynamic performance.

ACKNOWLEDGMENT

This work was supported by the National Science Council, Taiwan, R.O.C., under grant NSC 99-2221-E-027 -113 -MY3.

REFERENCES

[1] B. Zhang, Y. Li and Y. Zuo, "A DSP-based fully digital PMSM servo drive using on-line self-tuning PI controller", Proceeding of the 3rd Power Electronics and Motion Control Conference, vol. 2, Aug. 2000, pp. 1012-1017.

[2] Y. Guo, L. Huang, Y. Qiu, and M. Maramatsu, "Inertia identification and auto-tuning of induction motor using MRAS ", Proceeding of the 3rd Power Electronics and Motion Control Conference, Aug. 2000, pp. 1006-1011.

[3] K. Fujita and K. Sado, "Instantaneous speed detection with parameter identification for ac servo system", IEEE Transactions on Industry Applications, vol. 28, no. 4, Jul. 1992, pp. 864-872.

[4] K.B. Lee, J.H. Song, I. Choy, and J.Y. Yoo, "An inertia identification using ROELO for low speed control of electric machine", IEEE APEC, Feb. 2003, pp. 1052-1055.

[5] S. M. Yang, J. D. Lin, "Observer-Based Automatic Control Loop Tuning for Servo Motor Drive", The 10th IEEE International Conference on Power Electronics and Drive Systems, Kitakyushu, Japan, Apr. 22-25, 2013.

[6] M. De Campos, E.G. Caratti and H.A. Grundling, “Design of a position servo with induction motor using self-tuning regulator and Kalman filter”, IEEE IAS Annual Meeting, Oct. 2000, pp. 1613-1618.

[7] S. Morimoto, M. Sanada, and Y. Takeda, “Mechanical sensorless drives of IPMSM with online parameter identification”, IEEE Transactions on Industry Applications, vol. 42, no. 5, Sep./Oct. 2006, pp. 1241-1248.

[8] C. Y. Wu, M. C., Mao, S. H. Tasi, “Characteristics measurement of direct-drive brushless DC motors without using dynamometers”, International Conference on Electrical Machines and Systems, Nov. 2009, pp.1-6.

[9] K. Lu, M. Vetuschi, P. O. Rasmussen, and A. E. Ritchie,”Determination of high-frequency d- and q-axis inductances for surface-mounted permanent-magnet synchronous machines”, IEEE Transactions on Instrumentation and Measurement , vol. 59, no. 9, Sep.2010, pp. 2376-2382.

[10] T. Boileau, N. Leboeuf, B. Nahid-Mobarakeh, and F. Meibody-Tabar, “Online identification of PMSM parameters: parameter identifiability and estimator comparative study”, IEEE Transactions on Industry Applications, Vol. 47, no. 4, Jul./Aug. 2011, pp. 1944-1957.

TABLE 1 COMPARISONS OF MANUAL AND AUTO-IDENTIFIED PARAMETERS

	Manual	Auto-identified	% Error
r_s (Ω)	2.32	2.64	13.8%
L_{qs} (mH)	5.45	4.99	8.3%
L_{ds} (mH)	4.38	5.25	16.6%
J (kg-m^2)	3.28x10^{-4}	3.46x10^{-4}	5.7%
B (Nm/rad/s)	2.33x10^{-3}	2.45x10^{-3}	5.3%
K_t (Nm/A)	0.486	0.478	1.5%

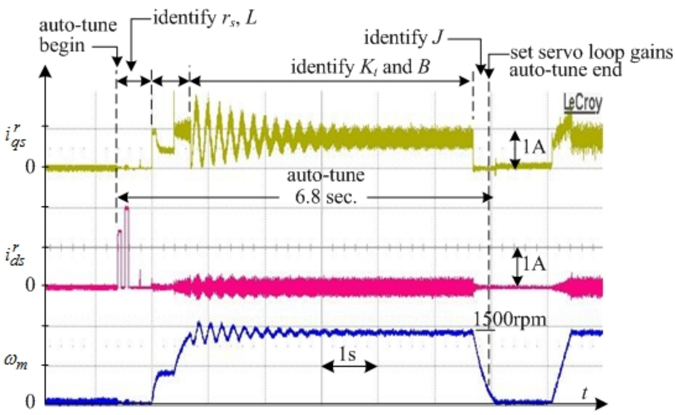

Fig. 9 Motor q- and d-axis currents, and speed waveforms for the auto-tune process, K_{p_v} and K_{i_v} during [t_3, t_4] are set to 0 and 1, respectively.

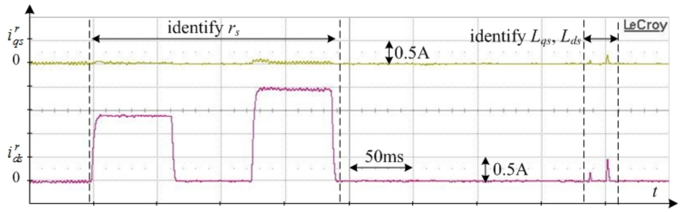

Fig. 10 Amplified view of the r_s and L measurements in Fig. 9.

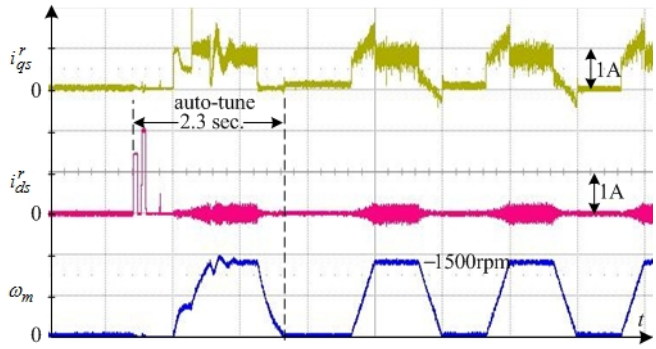

Fig. 11 Motor q- and d-axis currents, and speed waveforms for the auto-tune process, K_{p_v} and K_{i_v} during [t_3, t_4] are set to 0.016 and 1, respectively.

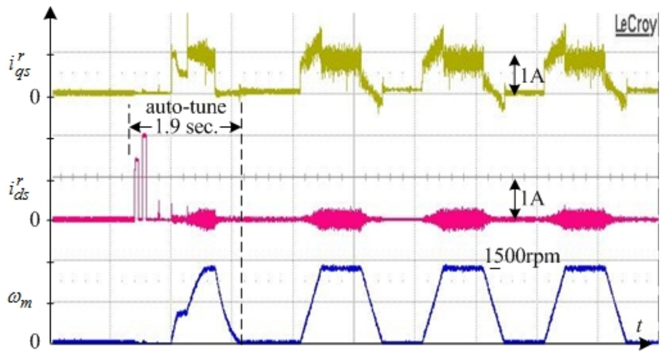

Fig. 12 Motor q- and d-axis currents, and speed waveforms for the auto-tune process, K_{p_v} and K_{i_v} during [t_3, t_4] are set to 0.16 and 10, respectively.